



16th International Symposium on District Heating and Cooling, DHC2018,  
9–12 September 2018, Hamburg, Germany

## Analyses of Axial Displacement Measurements from a Monitored District Heating Pipeline System

S. Hay<sup>a</sup>, F. A. Villalobos<sup>b</sup>, I. Weidlich<sup>c</sup>, I. Wolf<sup>d</sup>

<sup>a</sup>AGFW | Energy efficiency association for heating, cooling and CHP, Stresemannallee 30, Frankfurt am Main, 60596, Germany

<sup>b</sup>Catholic University of Concepción, Alonso de Ribera 2850, Concepción, Chile

<sup>c</sup>HafenCity University, Überseesallee 16, Hamburg, 20457, Germany

<sup>d</sup>enercity Netzgesellschaft mbH, Auf der Papenburg 18, Hannover, 30459, Germany

### Abstract

The need for understanding the response of district heating piping systems on temperature-driven loads to improve life-time analysis has led to the development of a monitoring programme. This programme includes the design of the connection of an instrumented section of piping within an operating district heating network. The design complies with the current European district heating recommendations and standards [1, 4]. There are different conditions under testing and minor differences in design of the sections causing different friction resistance in the bedding soil. The pipes' axial displacements are recorded in six positions along each of the sections of the pipeline. For the first time axial displacements of four similar buried preinsulated bonded pipes were measured under defined on-site conditions. This experimental setup allowed preliminary results of axial displacements, which are relevant for the district heating design, operation and maintenance. The contribution focusses on the results of the first period of operation, where a defined start-up procedure is performed (temperature increase up to 90 °C, held constant for 60 days). Afterwards the operating temperature was reduced down to the ambient temperature. The start-up procedure was repeated once before starting the cyclic-operating procedure up to 140 °C. The measured maximum pipes' axial displacements at operating temperature of 90 °C were around 25 mm in the bows of the monitored pipelines. The measurement results are between estimated values using current recommendation procedures (23 mm) and commercial computer programs (31 mm). In addition, residual displacements at ambient temperature level were measured. The impact of unloading-reloading cycles on pipe deformation behaviour will be a future research focus of the ongoing monitoring programme. The results of the four sections will be presented in a comparative way and a forecast on the cyclic-operating procedure will be given here.

© 2018 The Authors. Published by Elsevier Ltd.

This is an open access article under the CC BY-NC-ND license (<https://creativecommons.org/licenses/by-nc-nd/4.0/>)

Selection and peer-review under responsibility of the scientific committee of the 16th International Symposium on District Heating and Cooling, DHC2018.

\* Stefan Hay. Tel.: +49-69-6304-345, fax: +49-69-6304-455.

E-mail address: [s.hay@agfw.de](mailto:s.hay@agfw.de)

Keywords: district heating, buried preinsulated bonded pipes, pipe soil interaction monitoring, axial displacement

## 1. Introduction and Design

The monitored pipeline sections are based on four identical sections with constant coverage height of 0.8 m. Fig. 1 is a scheme of the all monitored pipeline sections. It shows the four sections having the same length properties ( $length_I = 5$  m,  $length_{II} = 41$  m). At the end of every section fixed point construction (here: execution as a concrete block) prevents mutual interference between the sections. During the design process the axial displacements as well as the relevant static conditions of the buried preinsulated bonded pipes of the monitored pipeline sections has been calculated according to European district heating recommendation and standard EN 13941 [1] with the calculation program sisKMR [2]. The four sections differ from each other due to different casing pipe connections, the number of casing pipe connections per section and the bedding material used. Table 1 shows the differences.

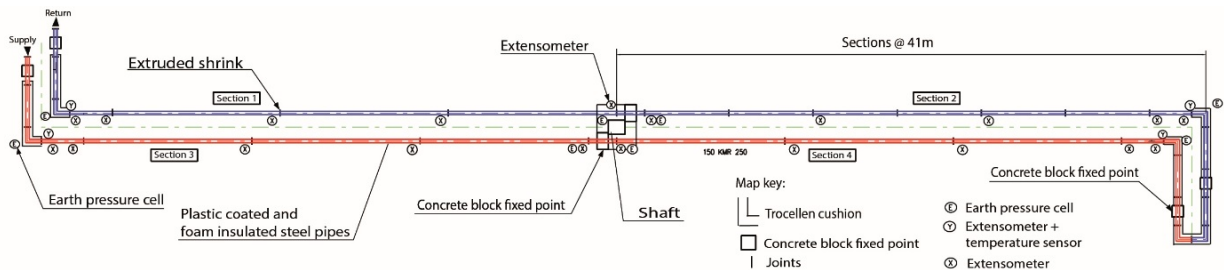


Fig. 1: Scheme of the monitored pipeline sections, showing fixed points, joints and cushions

Table 1. Differences between sections 1-4 (bedding material, type and number of jacket pipe connections).

Section	Bedding Soil Type	Type of Joints	Number of Joints
1	Sand	Extruded shrink	5
2	Sand	Plastic shrink-on sleeves	8
3	Sand	Plastic shrink-on sleeves	5
4	Sand / Gravel	Plastic shrink-on sleeves	5

To measure the soil-pipe interaction, the four sections are equipped with the same number of extensometers (axial displacement sensors, deviations in the measurement result  $\pm 0.1$  mm). The positioning of the measuring sensors is carried out in the same way for all sections (see fig. 1). In all sections, the last joint in front of the bows of the monitored pipelines is not filled with foam. The resulting cavities are used to install measurement equipment, consisting of an extensometer sensor and a temperature sensor, which are fixed at the steel medium pipe. Due to the variation of the bedding soil as well as the variations of joints (system and number) it can be assumed that the frictional forces between the pipeline and the surrounding soil develop differently in the four sections. This has an effect on the axial displacement of the sections as well as on the stress of the insulated pipes. For the dimensioning of insulated pipes, assumptions are made for the degree of compaction and the coefficient of friction  $\mu$  on the basis of the bedding soil used. Depending on the type of joints and the conditions during the assembly process of the joints, an increase of the diameter of the pipe segment can occur. Both the increase of diameter in the region of the joints and the deviations of the friction conditions resulting from the bedding situation are not included in the calculation. These, however, affect the stress of buried insulated pipes and are necessary for a deeper understanding of the construction as well as more detailed predictions regarding the service life in district heating systems.

### 1.1. Research objectives and related operations

In the dimensioning process of insulated pipes in district heating systems, the fatigue check is based on the Palmgren-Miner approach according to the current recommendations and standards [1, 3]. In these norms and standards, real temperature loads are converted into the equivalent number of full temperature cycles (FTCs) and limited to a certain number of presupposed FTCs. According to the dimensioning of the monitored pipeline section [1, 3], the 250 FTCs used for material fatigue are generated in total in six different operating phases (phase 0: defined start-up procedure 1 FTC; phase 1 to 4: 50 FTCs per phase; phase 5: 49 FTCs) during the entire monitoring programme. The connection to the district heating network of the utility company inetz GmbH (located at Chemnitz, Germany) and the regulation of the supply temperature in accordance with the defined operating program are made via a specially designed connecting station in the measuring container. According to the intended mode of operation of the respective operating phase, the supply temperature between 60 °C and 140 °C is regulated by the connecting station. After completion of the research operation, parts of the pipelines will be subjected to destructive tests in material testing institutes. In order to verify the material degradation due to the 250 FTCs, the initial values of the delivered material were determined on a brand new straight 12 m pipe (DN 150) according to EN 253 [4]. The comparison of the determined material parameters, before and after the load, enables to quantify the degradation of the material on the basis of the applied load. In this paper the results of phase 0 are presented and interpreted. The operating phase 0 can be subdivided into the following 3 partial operating phases.

Sub-operating phase 01 (SOP01): In operating phase 0, the research measuring section was first filled via the return line of the heating network. Subsequently, the operating temperature of the monitored pipeline sections was raised to 90 °C with a gradient of 5 K/h. The operating temperature 90 °C was held constant over 61 days.

Sub-operation phase 02 (SOP02): Subsequently, the heat supply was interrupted for a period of 30 days and the monitored pipeline sections cool down to the temperature level of the surrounding soil via natural convection.

Sub-operating phase 03 (SOP03): In the last sub-phase of operating phase 0, the monitored pipeline sections were reheated to an operating temperature of 90 °C. Initially, the minimum operating temperature was set via the connecting station while the target temperature of 90 °C was subsequently realized with a gradient of 5 K/h. The operating temperature of 90 °C was held constant for another 30 days.

After completion of the entire monitoring programme, it will be possible to compare different modes of operation and, based on this to assess their influence on the service life time of the monitored pipeline sections. Based on the results, it can be expected that improved approaches will be incorporated into the calculation of material fatigue.

## 2. Diameter measurements and geotechnical investigations

### 2.1. Diameter increase of the joints

To determine the influence of the increase of diameter of the various joints or number of joints, the peripheries of the joints were measured and documented after the installation. In fig. 2, the embedded extrusion sleeve is shown during the assembly process of section 1. At the construction site, this joint is adapted to the preinsulated pipes and welded by means of polyethylene (PE) welding. As shown in fig. 2, production-related PE circular welds are created at both ends of the sleeve, as well as a PE longitudinal weld in the middle of the joint. Depending on the diameter of the insulated pipes, these PE welds lead to an increase in diameter at the joints. The diameter in the middle of the jacket pipe connection is 250 mm and thus 3.6 mm smaller than the outside diameter of the insulated pipe (253.6 mm). The circular PE welds cause a diameter, which are between 259.4 mm and 267.4 mm and thus compared to the outer diameter of the insulated pipe to a diameter increase between 5.8 mm and 13.8 mm.



Fig. 2: Embedded extrusion sleeve section 1 after the production of the PE welds and the foaming process

In the same way as for section 1, the geometrical parameters of the remaining joints of sections 2 to 4, which were designed as shrink-on sleeve joints with additional shrink sleeves, were documented after their assembly. For sections 2 to 4, the same diameter (283.4 mm) was measured for all shrink sleeves. The installed shrink sleeves have a 29.8 mm larger outer diameter compared to the insulated pipes (253.6 mm).

## 2.2. Results of geotechnical investigations

Fig. 3 shows the particle size distribution of the bedding materials for the sections 1 to 3 (blue) and section 4 (purple). These bedding materials are oriented towards permissible limit curves of the current draft standard for the construction of buried preinsulated bonded pipes - prEN 13941-2, 2016 [5]. It can be seen that the bedding material of section 4 consist of 50% coarse grain fraction (higher than 1 mm). On the other hand, in the case of sections 1 to 3, 60% of the bedding is sand (grain size lower than 0.2 mm).

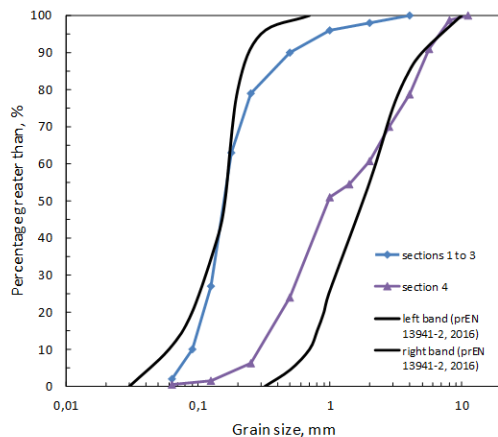


Fig. 3: Grain size distribution of the bedding materials in section 1 to 3, and in section 4 following prEN13941-2, 2016 [5]

The bedding materials used were examined both in the laboratory and in the field with regard to their properties and the installation situation in order to determine the relevant parameters for the interpretation of the measurement results. In the laboratory experiments characteristic mechanical parameters of the soil as well as the relative density were determined. Friction coefficients  $\mu_{\max} = 0.504$  and  $\mu_{\text{residual}} = 0.415$  were determined for the bedding material of the section 1 to 3 for the relative density of 0.4. For section 4, the maximum coefficient of friction is  $\mu_{\max} = 0.468$  and a residual friction value of  $\mu_{\text{residual}} = 0.429$  was determined for the same relative density of 0.4 [6].

## 3. Measurement results of the operating phase 0

### 3.1. Section 3

The section 3 corresponds to the conventional construction of insulated pipes for district heating in Germany and thus forms a reference route to real district heating networks. Consequently, section 3 is best suited for a detailed analysis and presentation of the measurement results. In fig. 4, the measurement results from the entire operating phase 0 for section 3 are shown. Fig. 4 clearly shows the three partial operating phases based on the temperature and displacement measurements.

Before the first filling on April 27, 2017, the measuring sensors were zeroed. Subsequently, section 3 was put into operation in accordance with the starting process described in SOP01 and operated according to the operating criterion of phase 0 (SOP01, SOP02, SOP03). Regarding the curve progression of the axial displacements in fig. 4 it can be noted that they qualitatively follow the curve progression of the operating temperature of section 3. Besides that the measured displacements increase over the sections length. Correspondingly, displacements are at a minimum of 1.5 m from the fixed point (in the middle of the monitored pipe sections, measured on S311.5 sensor). The sensor on the steel medium pipe (S3140), which is 40 m away from the fixed point, measures the largest axial

displacements and reaches a maximum value of 25.8 mm in operating phase 0. The measured axial displacements on the steel medium pipe (S3140) are approx. 1.5 mm larger than those on the adjacent measuring point (S3139,4) on the PE jacket of the insulated pipe which has a distance of 39.4 m to the fixed point in the middle.

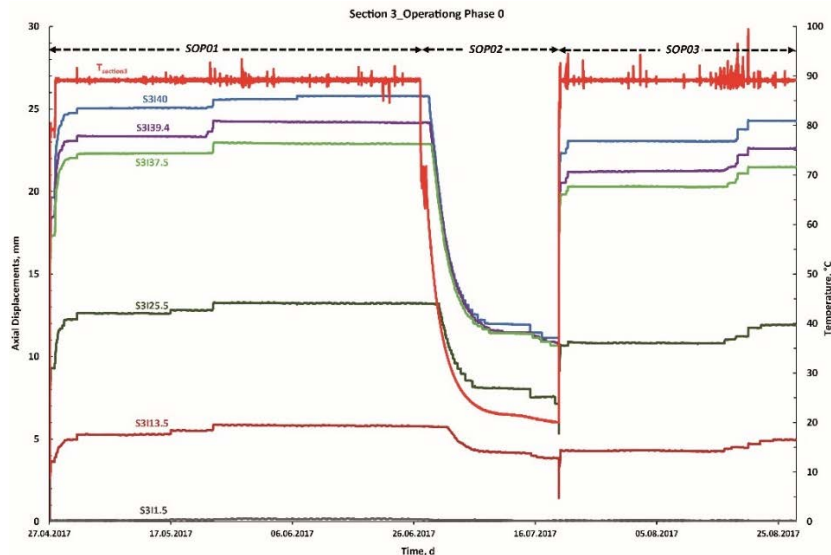


Fig 4: Measuring results of section 3, temperature and axial displacements versus time

In the SOP01, which lasts from April 27 to June 27, 2017, the measurements of the axial displacements seem to have larger changes at a total of three times: Mai 01, Mai 17, and Mai 24, 2017. Looking more closely at these times, it can be stated that minor positive temperature increases between 2 K and 5 K on Mai 01 and Mai 24, 2017 cause axial displacements at all six extensometers. The associated displacements range between 0.2 mm and 0.6 mm. On Mai 17, 2017 axial displacements occur at the sensors S3113.5 and S3125.5. Compared with the axial displacements in the first 72 h of the SPP01 (the displacements increase from 0 mm to 20 mm) these measured displacements are significantly smaller. Temperature reductions in the comparable amplitude between 2 K and 5 K show no measurable axial displacements.

Fig. 5 (see p. 6) shows the first 72 h of the defined starting procedure and the associated measurement results of section 3. As can be seen in Fig. 5, the operating temperature during the filling process suddenly increases from about 10 °C to about 65 °C. Due to the minimum possible temperature level at this time, the temperature of the sections were first raised to 80 °C and then at the intended rate of temperature change of 5 K/h to 90 °C which were reached after 24 h. Fig. 5 shows the detailed course of the axial displacements during the first 72 hours of operation. It can be seen that after reaching the target temperature of 90 °C (after 24 h), a large part of the axial displacements are formed. In addition, fig. 5 shows that creep processes occur after 24 h without any further increases in the track temperature, which almost completely stop after 72 h.

Table 2 (see p.6) shows the measurement results at selected times of the extensometer sensors and the supply temperature - measured on steel medium pipe - of section 3. The first value of the displacement measurement in table 2 indicates the absolute axial displacement of the measuring point (specified in mm) in each case at the time of measurement. The bracketed values represent the percentage of the displacement achieved at the time of measurement, relative to the maximum value of the axial displacement that this measuring point reaches after 61 d.

The tabular overview once again confirms the results already described in fig. 5. Table 2 shows for section 3, that after one operating hour axial displacements occur, which are 50% of the maximum value in operating phase 0. The track temperature at 62.3 °C is still below the target temperature. Looking at the track temperatures in table 2 the measurement results with max. 89.2 °C are still below the set point temperature of 90 °C, while the temperature sensors of the sections measure the temperature of the steel (outside of the steel medium pipe). The associated temperature deviation is reflected in the temperature measurement results shown. After one day, the axial

displacements increased to over 80% measured at sensors further away than 13.5 m from the fixed point in the middle. The measuring point S3I13.5 has even smaller displacements with 67%. On the S3I1.5 sensor, very small displacements have been measured over the entire period of observation. In the following 2 days, the axial displacements increase at constant supply temperature to over 90%. These creep processes can also be clearly seen in fig. 5. On the basis of a tabular overview, it is also clear that the creeping processes are largely completed after 72 h (3d).

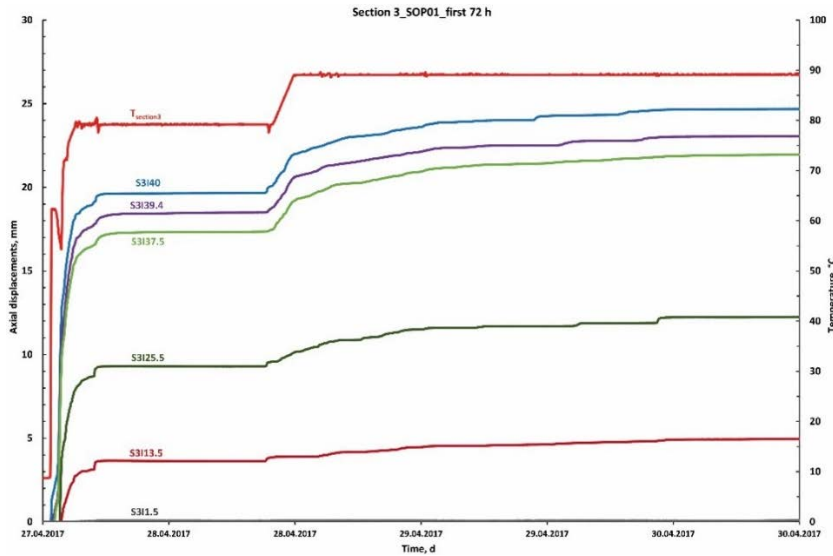


Fig. 5: Measuring results SOP01 (first 3 days of operation), temperature and axial displacements versus time

Table 2. Measurement results of section 3 at selected points in SOP01

Time	T <sub>Section3</sub> [°C]	S3I1.5 [mm]	S3I13.5 [mm] (%)	S3I25.5 [mm] (%)	S3I37.5 [mm] (%)	S3I39.4 [mm] (%)	S3I40 [mm] (%)
1h	62.3	0.0	0.4 (7)	4.0 (30)	10.1 (44)	11.3 (47)	13.0 (50)
1d	89.2	0.0	3.9 (67)	10.3 (84)	19.4 (85)	20.8 (86)	22.1 (86)
2d	89.1	0.0	4.7 (81)	11.7 (89)	21.5 (94)	22.5 (93)	24.3 (94)
3d	89.1	0.1	5.0 (86)	12.3 (93)	22.0 (96)	23.0 (95)	24.7 (96)
4d	89.1	0.1	5.0 (86)	12.3 (93)	22.0 (96)	23.1 (95)	24.8 (96)
61d	89	0.1	5.8 (100)	13.2 (100)	22.9 (100)	24.2 (100)	25.8 (100)

Fig. 6 (see p. 7) shows the cooling behavior of section 3 and the associated displacements. After the monitored pipe sections were put out of operation on June 27, 2017 by turning off the flow pump, further temperature increases were measured in the course of the temperature. These are also shown in fig. 6 and are due to flow processes that result from the pressure and temperature differences to the connected district heating network. As a result, the manual shut-off valves were closed on June 28, 2017 and the monitored pipe sections were thus completely disconnected from the heating network. Afterwards, the operating temperatures of section 3 - as shown in fig. 6 - declined.

Initially, a temperature drop of 30 K is necessary before section 3 starts to shift back towards 0-position. In an analogous manner to the starting process, the sensors with the greatest distance to the fixed point also begin to reverse the axial displacement when the temperature is decreased. Thus, the values of the sensors S3I40, S3I39.4 and S3I37.5 have reduced to less than 20 mm before the sensors 25.5 m and 13.5 m start to move. Until July 06, 2017, the displacements have receded to less than 13 mm.

In table 3 (see p.7), in an analogous manner as in table 2, the axial displacements of the measuring points of section 3 at the respective times are given. The results presented in table 3 demonstrate that the first reduction in

axial displacement at S3I40 occurs after 36 hours, in conjunction with a 29.9 K reduction in track temperature. 24 hours later, the section temperature cooled by further 12.5 K and as a result, the displacements of the sensors S3I40, S3I39.4 and S3I37.5 are reduced to approximately 90%. On the sensors S3I25.5 and S3I13.5, no reduction of the displacements occurred at this time. The numerical values show that the axial displacements in SOP02 are reduced to approximately 45% of the maximum measurement result of the respective sensor (at 90 °C). The tabular overview uses the numerical values to clarify the results already derived from fig. 6.

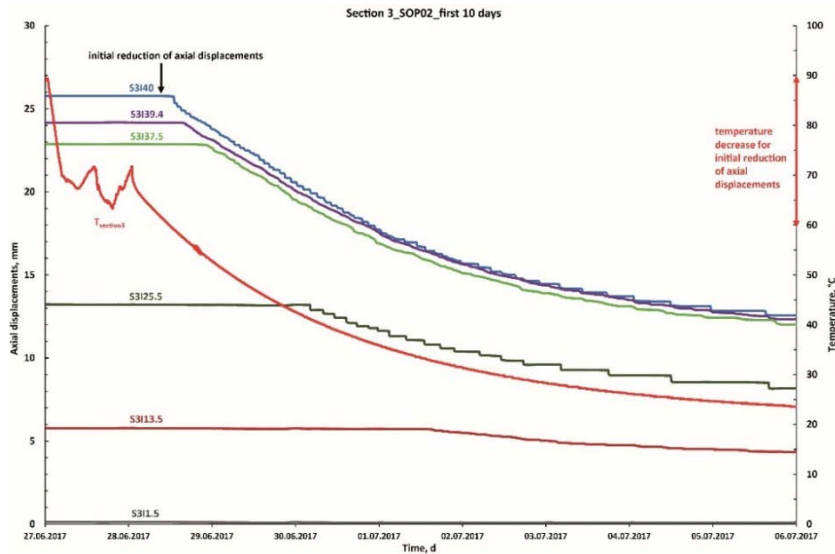


Fig. 6: Measuring results SOP02 (first 10 days), axial displacements and decrease of supply temperature versus time

Table 3. Measurement results of section 3 at selected point in SOP02

Time	T <sub>Section3</sub> [°C]	S3I1.5 [mm]	S3I13.5 [mm] (%)	S3I25.5 [mm] (%)	S3I37.5 [mm] (%)	S3I39.4 [mm] (%)	S3I40 [mm] (%)
61d	89	0.1	5.8 (100)	13.2 (100)	22.9 (100)	24.2 (100)	25.8 (100)
61.5d	70.8	0.1	5.8 (100)	13.2 (100)	22.9 (100)	24.2 (100)	25.8 (100)
62.5d	59.1	0.1	5.8 (100)	13.2 (100)	22.9 (100)	24.2 (100)	25.5 (99)
63.5d	46.6	0.0	5.8 (100)	13.2 (100)	21.0 (92)	21.5 (89)	22.2 (86)
64.5d	38.5	0.1	5.7 (98)	12.4 (94)	18.1 (79)	18.6 (77)	19.0 (74)
77.5d	21.6	0.1	4.2 (72)	8.0 (61)	11.4 (50)	11.5 (48)	11.9 (46)
84d	20.1	0.1	3.8 (66)	7.1 (54)	10.7 (47)	10.7 (44)	11.1 (46)

The defined reheating procedure to the supply temperature of 90 °C in SOP03 starts on July 20, 2017 on the basis of the corresponding residual axial displacements of the different measuring points in section 3 (see p.8, fig.7). The supply temperature of the monitored pipe sections is determined by the temperature level of the return line of the district heating system, which varies between 75 °C and 93 °C during the day on July 20, 2017. It is only in the late afternoon that it is possible to compensate for the network-related temperature fluctuations in such a way that the control regulates the defined operating state (90 °C) with the temperature change rate of 5 K/h. As shown in fig. 7, most of the axial displacements occur within the first 12 hours after the section restarts. As a result of temperature fluctuations on July 21, 2017 a further increase in the axial displacements is observed. It cannot be ruled out that without these temperature pulses, the axial displacements could have reached a stationary state after only 24 h.

Table 4 (see p. 8) shows the absolute values of the axial displacements as well as the percentage values related to the maximum measured value of the respective sensor (after 61 d) at selected times of SOP03. It can be seen that the measurement results increase within the first hour after reheating section 3 to about 70% of the maximum displacements. Compared with the same period during the first start (SOP01), the measurement results (84.05 d) are thus about 20% above the displacements after 1 hour, whereby the supply temperature at the time shown in table 4 is

20 K higher. Two days after restart, both the supply temperature and the axial displacements have reached a stable state. The axial displacements have been set at a level of 90% of the maximum displacements in SOP01. Regarding fig. 7 and table 4, it should be noted that the axial displacements - compared to the startup process of SOP01 – form in a similar speed but the creep processes observed in SOP01 hardly take place or stop after only 48 hours.

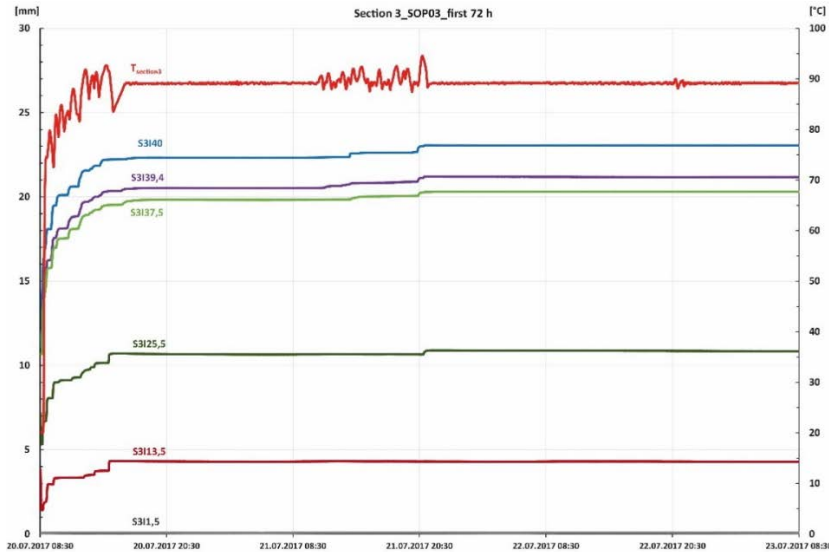


Fig. 7: Measuring results SOP03 first 72 hours of the reoperation, axial displacements and supply temperature

Table 4. Measurement results of section 3 at selected point in SOP03

Time	T <sub>Section3</sub> [°C]	S311.5 [mm]	S3113.5 [mm] (%)	S3125.5 [mm] (%)	S3137.5 [mm] (%)	S3139.4 [mm] (%)	S3140 [mm] (%)
84d	20.1	0.1	3.8 (66)	7.1 (54)	10.7 (47)	10.7 (44)	11.1 (46)
84.05d	79.1	0.1	2.9 (50)	8.1 (61)	15.8 (69)	16.3 (67)	18.1 (70)
85d	89.2	0.1	4.3 (74)	10.7 (81)	19.8 (86)	20.5 (85)	22.3 (86)
86d	89.1	0.1	4.3 (74)	10.9 (83)	20.3 (89)	21.2 (88)	23.1 (90)
91d	89.2	0.1	4.3 (74)	10.8 (82)	20.3 (89)	21.2 (88)	23.1 (90)
123d	89.1	0.1	5.0 (86)	11.9 (90)	21.5 (94)	22.2 (92)	24.3 (94)

In the period between July 21 and August 16, 2017, the supply temperatures of sections 3 are subject to fluctuations, which in some cases are to be quantified as more than 5 K. Nevertheless, no further displacements occur during this period. This suggests that after the reheating procedure (SOP03) of the operating phase 0, very stable stationary states have been already formed at the beginning. In mid-August 2017, the operating temperature deviates up to 10 K in places from the set point temperature of 90 °C. These generate a further increase in the displacement measurements. Due to the time overlay, it can be demonstrated that the axial displacements - shown in fig. 4 (see p. 5) - are due to the temperature pulses at the end of August 2017 and that otherwise the defined termination criterion for operating phase 0 ( $\Delta l \rightarrow 0$ ) was met. On the basis of this, it was decided to move to cyclic operation phase 1 on August 27, 2017.

### 3.2 Comparison between the measurement results of all sections and the calculations of design

The curve progression of temperatures and axial displacements shown on the results of section 3 are also reflected qualitatively in the curve progressions of sections 1, 2, and 4. In the following, the previously described extreme positions of the three partial operating phases are compared and set in relation to the calculation results of the static design. During the dimensioning, the axial displacements were determined according to the laying and



operating temperatures according to the valid calculation formulas regarding [1]. The influences of the different bedding soils are essentially taken into account in the calculation on the basis of the coefficient of friction  $\mu$ . It was assumed that a friction coefficient  $\mu = 0.4$  was achieved for the sand bedding of sections 1, 2 and 3, and realistic results for section 4 with a higher coefficient of friction  $\mu = 0.5$ .

Table 5 shows the calculation results with sisKMR [2] based on [1] with the different friction values for the measurement points at 90 °C track temperature (see Calculation1 and Calculation2). The maximum axial displacements of the various sections of the monitored pipe sections after 61 days before the lowering of the operating temperature are included as percentages based on the calculation results 1 with the friction coefficient  $\mu = 0.4$  in table 5. The values in brackets of table 5 refer to the results of calculation 2, in which the friction coefficient is  $\mu = 0.5$ . The representation selected in table 5 enables us to compare the measurement results of the individual sensors of the different sections at the same measuring points.

Table 5. Measurement results after 61 days of operation of all sections in percent referred to the results of calculations

Section	T <sub>Section</sub>	SI1.5	SI13.5	SI25.5	SI37.5	SI39.4	SI40
1	88 °C	30% (50%)	64% (88%)	72% (92%)	72% (85%)	76% (89%)	74% (87%)
2	88.8 °C	133% (200%)	65% (89%)	69% (88%)	73% (86%)	73% (86%)	77 (90)
3	89 °C	17% (255)	66% (91%)	72% (92%)	79% (93%)	78% (92%)	82 (96)
4	87.8 °C	0 (0)	40% (55%)	59% (75%)	66% (78%)	72% (84%)	73 (86)
Calculation1 ( $\mu=0,4$ )	90 °C	0.6 mm	8.8 mm	18.3 mm	29.0 mm	30.9 mm	31.4
Calculation2 ( $\mu=0,5$ )	90 °C	0.4 mm	6.4 mm	14.4 mm	24.5 mm	26.4 mm	26.9

It can be stated that the calculation results of calculation 2 with the higher coefficient of friction are closer to the measurement results of all partial sections. The deviations between the measurement results of the sections and the calculation results of calculation 2 are sometimes even less than 10%. In addition, the measurement results of the sections 1, 2 and 3 are usually less than 10% from each other. For section 4, the deviations from the measurement results of the other sections at the measuring points 40 m and 39.4 m are also in the range of 10% deviation. Between the measuring points 37.5 m and 1.5 m, these deviations increase to more than 25%.

Table 6. Measurement results after 84 days of operation of all sections in percent referred to the results of calculations

Section	T <sub>Section</sub>	SI1.5	SI13.5	SI25.5	SI37.5	SI39.4	SI40
1	20,6 °C	33% (33%)	97% (75%)	103% (74%)	126% (87%)	145% (102%)	155% (109%)
2	20 °C	200% (200%)	132% (102%)	153% (110%)	138% (95%)	187% (132%)	203% (143%)
3	20,1 °C	33% (33%)	103% (79%)	118% (85%)	155% (107%)	151% (106%)	156% (110%)
4	20,8 °C	0,0	76% (58%)	90% (64%)	139% (96%)	151% (106%)	177% (125%)
Calculation1 ( $\mu=0,4$ )	10 °C	0.3 mm	3.7 mm	6.0 mm	6.9 mm	7.1 mm	7.1 mm
Calculation2 ( $\mu=0,5$ )	10 °C	0.3 mm	4.8 mm	8.4 mm	10 mm	10.1 mm	10.1 mm

Table 6 shows - in the same way as table 5 - the calculation results with sisKMR [2] based on [1] with the different friction values for the measuring points at 10 °C section temperature - for the state of a cooled pipe. Based on the numbers in table 6, the measurement results of the individual sensors of the different sections will be compared at the same measuring points. In summary, first it can be stated that both in the calculation results as well as in the measurement results of the four sections, the states do not shift back to 0-position and there is a residual displacement. In addition, it should be noted temperatures of the sections at the specified measuring time are 10 K above the temperature assumptions of the calculation. It is therefore not surprising that the residual displacements of the sections are usually larger than those of the calculations. The tabular overview also makes it clear that the deviations of the residual displacements of the sections to the calculation results also increase with increasing length of the sections. Unlike the presentation in table 5, the results of SOP02 (see table 6) are much more different. This can be seen particularly clearly on Section 2.

In table 7 the sensors' maximum measured results in SOP03 referred to the maximum value – measured at the end of SOP01 - are shown. Except S2I1.5 no sensor achieved the maximum axial displacement of SOP01. As shown in table 7 the differences in the results per section decreases with the total length of the sections. The results of axial displacement in SOP03 are in the range of 90% of the maximum in SOP01.

Table 7. Comparison sensors axial displacement SOP03 with maximum measurements SOP01

Section	SI11.5	SI13.5	SI25.5	SI37.5	SI39.4	SI40
1	50%	75%	81%	90%	91%	90%
2	100%	84%	89%	91%	92%	94%
3	56%	86%	90%	94%	93%	94%
4	0	74%	76%	86%	85%	92%

#### 4. Conclusions

In this paper the axial displacements of four monitored pipeline sections achieved during the first period of operation at 90 °C were presented. The measuring results in SOP01 and SOP03 are showing that the predominant share of axial displacements were achieved during the first 24 h of operation caused by the temperature increase. Up to 72 h extend creeping was noted before steady stress conditions in the pipe-soil interaction were achieved. Small temperature increases could disturb this steady stress conditions and cause an increase of the measured displacement. Temperature decreases in the same range do not lead to a reduction of the axial displacements. It was shown that in the beginning of SOP02 an initial temperature decrease of 30 K is needed to disturb the steady stress conditions in the pipe-soil interaction and that the insulated pipe do not shift back to 0-position. The measured residual displacement was in the range of 40% of their maximum values. Starting from the residual displacements in SOP03 smaller displacements were achieved. Although the supply temperature in SOP03 differs more from the set temperature the measurements are more stable compared with the results of SOP01 which indicate on more stable pipe-soil stress conditions.

The results of the geotechnical investigations provide us with higher friction values compared to the standards. The diameter of the joints are compared to the diameter of the insulated pipes only 15 mm higher. Regarding the calculations referred to the results of the measurements larger compliance with higher friction coefficient  $\mu = 0.5$  was achieved. This is in line with the results of the geotechnical investigations. Nevertheless, there is still a deviation around 10% between the measurement results and the result of calculation 2. This could be due to the diameter increase of the joints. The minor differences in the design of the sections have not caused a significant deviation in the measuring results during the operating phase 0. It is expected that in operating phase 1 the higher temperatures and the cyclic procedures will enlarge the resistance in bedding soil. This should lead to a higher differences in the measuring results of the axial displacements of the four sections. On the basis of the presented measurement results it could be shown that the pipelines are exposed to a very high initial load due to the starting process. This should be verified in further researches and taken into account in the pipe deformation behavior as well as in the material fatigue of buried preinsulated bonded pipes.

#### Acknowledgements

This work is part of ongoing research programmes on district heating by AGFW for the development and improvement of pipeline networks. The authors are especially grateful to the BMWi German Federal Ministry of Economics and Energy for the funding support to these ongoing research programmes (funding code: 03ET13335).

#### References

- [1] EN 13941 (2010). Design and installation of preinsulated bonded pipe systems for district heating. European CEN, Brussels.
- [2] sisKMR (2016). District heating pipe stress analysis software. Version 24.9.0. GEF Ingenieur AG, Leimen, Germany.
- [3] AGFW FW 401 (2007). Installation and calculation of preinsulated bonded pipes for district heating networks. Part 10: Static design; basics of stress analysis. AGFW, Frankfurt am Main.
- [4] EN 253 (2015). District heating pipes - Preinsulated bonded pipe systems for directly buried hot water networks - Pipe assembly of steel service pipe, polyurethane thermal insulation and outer casing of polyethylene. European CEN, Brussels.
- [5] prEN 13941 (2016). District heating pipes – Design and installation of thermal insulated bonded single and twin pipe systems for directly buried hot water networks: Part 1: Design. Part 2: Installation. European CEN, Brussels.
- [6] IGtH (2015). Geotechnische Untersuchung des Bettungsmaterial der FW-Langzeitmessstelle. Institute for Geotechnical Engineering Leibniz University Hannover, Hannover.